The Effect of Slit Orientation and Length on the Tear Behavior of S8210 Used for Freight Wagons Tarpaulin

Liviu D. Pirvulescu
Associate Proffesor
University of Timisoara
Faculty of Mechanical Engineering
Romania

Dan I. Stoia
Associate Proffesor
University of Timisoara
Faculty of Mechanical Engineering
Romania

Ilare Bordeasu
Full Professor
University of Timisoara
Faculty of Mechanical Engineering
Romania

PVC-coated fabrics are widely used in tarpaulin applications due to their durability and flexibility. This study investigates the tearing behavior of PVC-coated fabric specimens containing central straight and inclined slits, sampled from S8210-type tarpaulins used in freight wagons. Uniaxial tensile tests were performed on both intact and slit specimens. Horizontal slits having lengths of 5, 10, and 20 mm, as well as inclined slits of 20 mm at 30°, 45°, and 60° angles, were analyzed. The results reveal two distinct fracture modes: progressive and abrupt failure. Inclined slits exhibited a progressive, Z-shaped crack propagation pattern while the horizontal slits lead to a more sudden failure. Key fracture parameters, including maximum fracture force, fracture energy, and the influence of slit geometry on fracture strength, were determined. A critical opening length beyond which the tarpaulin's repair is recommended was also identified.The paper translates the theoretical concepts of breaking energy in a directly measurable parameter (a_{ech}). This can be investigated directly on site by the maitainence personeell and based on the reading and proposed tables for this material, cand make safety decisions.

Keywords: *tarpaulin, tensile strength, breaking energy, horizontal slit, oblique slit, slit opening.*

1. INTRODUCTION

S8210 tarpaulins used for freight wagons are manu–factured in a variety of colors and patterns, represent low-cost, flexible, and easily fabricated textile com–posite membranes. Due to these characteristics, they are widely employed in sectors such as transportation, con–struction, agriculture, and maritime applications. Their widespread use is primarily determined by the ma–terial's resistance to environmental factors (e.g., wind, rain, snow) and by its intrinsic properties [1,2]:

- mechanical robustness: evaluated in terms of strength to tensile failure and abrasion under harsh con–ditions, originally designed for railway transport appli–cations;
- waterproofness: the PVC coating provides an effective barrier against water and moisture, making it suitable for outdoor covering applications;
- UV resistance: typically treated for protection against solar radiation this property is preventing rapid material degradation;
- dimensional stability: the ability to maintain shape and tensioning under varying environmental conditions.

In industrial practice, two main types of tarpaulins are employed [3]: one made of polytetrafluoroethylene (PTFE) coated fabric reinforced with glass fibers, and the other made of polyvinyl chloride (PVC) coated fabric reinforced with polyester fibers. Both materials consist of an open-weave network of orthogonal fibers coated on both sides [3].

PTFE fabrics are suitable for large-scale structures subjected to extreme loads and exhibit good fire resistance and high-temperature performance. A major drawback however is that glass fibers are brittle and difficult to fold, which can lead to a deterioration of the material's mechanical properties.

PVC-coated polyester fabrics are more commonly used due to their high cost-effectiveness compared to other tarpaulin types, such as those coated with rayon, silicone, or PTFE [4]. During their service life, improper installation and the variable loads imposed by external factors (natural or otherwise) can lead to the formation of cracks within the fabric structures. These cracks may propagate under relatively low external loads, ultimately resulting in material failure. Consequently, in recent years, experimental research investigating the influence of crack type on the strength of tarpaulins under different loading conditions has intensified.

Notable results were reported by Zhang et al. [5] on MC13122-type PVC tarpaulin with an initial horizontal notch and circular defects. Further important findings were obtained by Sun et al. [6] on PVC tarpaulin manufactured by Jiangsu VEIK Technology @ Material Co. Ltd, investigating initial horizontal cracks ranging from 5 to 50 mm, as well as inclined cracks. Analysis of these studies indicates that specimens with central cracks exhibit distinct crack propagation characteristics, with real structural deterioration observed in terms of stress distribution and crack opening patterns.

Other researchers [7–9] have investigated the effect of straight and inclined cracks on the tensile strength of

Received, April 2026, Accepted: June 2026
Correspondence to: Stoia Dan Ioan, University of Timisoara, Faculty of Mechanical Engineering, Mihai Viteazu 1, 300222 Timisoara, Romania
E-mail: dan.stoia@upt.ro
doi: 10.5937/fme2603475P

PVC- and PTFE-coated fabric tarpaulins. Based on their findings, these studies characterized the fracture pro–cesses of central cracks and determined the maximum load-bearing capacity of the cracked specimens.

Purnomo et al. [12] investigated the fracture tough–ness and deformation behavior of zeolite (Z)/high-den–sity polyethylene (HDPE) composites reinforced with chopped silk fibers (SF), which were distributed thro–ughout the thickness of the composite mixture. Sabok–takin et al. [13] analyzed the tensile, shear, and stretc–hing behavior of textile structures subjected to axial and multiaxial mechanical loading, loading conditions that are representative of those experienced by tarpaulins under wind action or snow loads. Saghafi et al. [14] studied the impact resistance of carbon- and glass-fiber-reinforced structures subjected to foreign-object impacts (e.g., stones and hail), while Dinulović et al. [15] pro–posed an innovative and efficient solution for the repair of damaged honeycomb structures.

Others work focus on the elastic properties of PVC foams subjected to uniaxial compressive loading were characterized using a full-field measurement metho–dology [16]. Zhang X. et al. [17] investigated the spe–cific mechanical properties of coated fabrics, including orthotropy, yarn density, and nonlinear tension beha–vior. Based on the energy balance theory and the Hedgepeth model for edge-notched specimens, they derived an incremental theoretical expression for the fracture toughness, Gc. Yu Y. et al. [18] examined the mechanical properties of polyvinyl chloride (PVC)-coated fabrics at elevated temperatures and after thermal exposure through uniaxial tensile testing. The test temperature range extended from 20 °C to 170 °C. Guo S. et al. [19] investigated the deformation behavior, energy dissipation mechanisms, and damage charac–teristics of four types of warp-knitted and weft-knitted PVC membrane materials by means of multi-stage cyclic loading experiments.

In line with the above-mentioned research, the present study investigates the tensile tearing behavior of S8210 PVC-coated polyester tarpaulin containing stra–ight and inclined slits of different lengths and orien–tations. While the concept of equivalent crack length has been previously reported for textile-reinforced com–posites, its applicability to S8210 freight wagon tar–paulins has not been investigated. The novelty of this work lies in the experimental validation of the equi–valent crack length approach for this material system, the correlation between equivalent crack length and re–sidual load-carrying capacity, and the assessment of its potential use as a practical parameter for maintenance and repair decisions in railway tarpaulin applications.

2. MATERIALSANDMETHODS

2.1 Material

The study was conducted on specimens of S8210 which is a high-performance polyester fabric core with a PVC coating, including a glossy lacquer on both sides.

It exhibits nonlinear, inelastic, and anisotropic behavior, resulting from contact friction nonlinearities between the constituent materials and the geometric irregularities of the corrugated base fabric structure [8].

The most important mechanical and structural pro–perties of the tarpaulin, according to the technical data–sheet provided by S.C. Satimpex SRL, are presented in Table 1.

Table 1. Manufacturer specifications for the tested material [1]

Thickness (mm)	Fabric type	Density (g/m^2)	Temperature range (^0C)	Tensile strength	
				Warp	Weft
0.6	Polyester	800	-30 ÷ +70	2750N/ 5cm	2500N/ 5cm

The macro and microscopic a structure of the S8210 tarpaulin is shown in Figure 1.

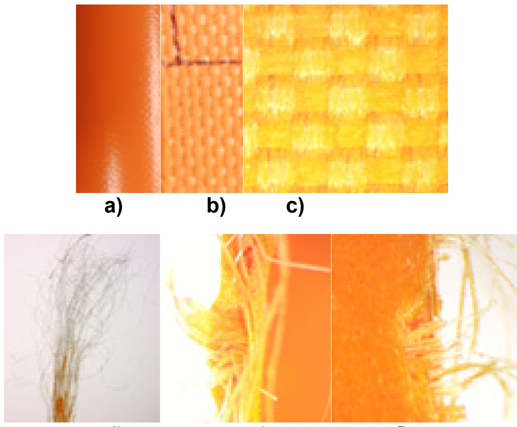

Figure 1. Tested material and macro and microscopic st–ructure: a) tested material; b) macroscopic image of the tarpaulin (10x); c) threads exposed (40x); d) yarns asse–mbly (40x); e) fracture cross-section 40x; fracture lateral view 40x

As shown in Figure 1, the tested material consists of a plain weave fabric coated with a layer of PVC (Figure 1a). The coated fabric contains seven yarns per centi–meter in both the warp and weft directions (Figures 1b and 1c). The cross-sectional shape of the warp and weft yarns is oval, and the yarns are periodically distributed in a wavy pattern (Figure 1c). Each warp and weft yarn are composed of multiple fine filaments, which together form the complete warp and weft yarns (Figure 1d).

2.2 Tests specimens and test configuration

The specimens were cut in the weft direction, in accordance with the requirements of BS EN ISO 1421:1998. To investigate the tearing properties, unia–xial tensile test specimens were prepared as strips with a length of L = 250 mm and a width of W = 50 mm. The active gauge length of the specimen (between grips) was L□ = 110 mm. The shapes of the specimens, both without cracks and with various initial straight and inclined cracks used for testing, are shown in Figure 2.

Seven sets of specimens were tested to minimize experimental errors, as follows:

- one set of specimens without cracks (see Figure 2a);
- three sets of specimens with a straight slit, perpendicular to the applied load F, with slit lengths 2a = 5, 10, and 20 mm (see Figure 2b);

- three sets of specimens with a constant slit length of 2a = 20 mm, inclined at angles of θ = 30°, 45°, and 60° relative to the horizontal direction (along the specimen width W) (see Figure 2c).

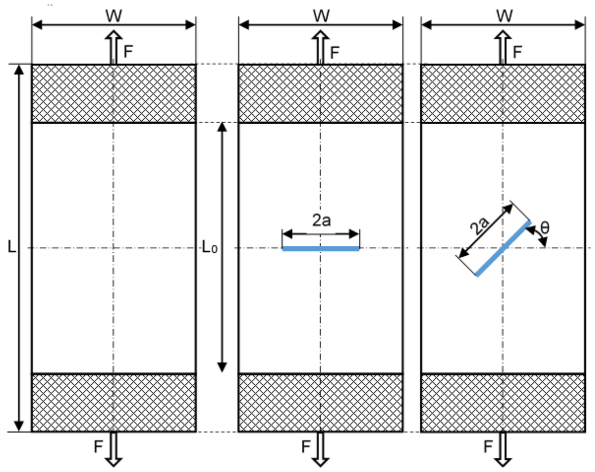

a) b) c)

Figure 2. Specimen configurations with different initial cra–cks: (a) no cracks; (b) horizontal crack (perpendicular to the direction of the force); (c) inclined crack (at an angle to the horizontal)

Each test set consisted of five specimens per case, and the mean value of the obtained results was adopted. Slits in the specimens were created using a surgical scalpel, under the stereo-microscopy magnification. The tests were conducted under ambient conditions, at a temperature of 22□°C and a relative humidity of 65□%.

Uniaxial tensile tests were performed using a Zwick/Roell Z005 universal testing machine (Figure 3a). The specimens were clamped using a custom-designed gripping device developed in-house to prevent specimen damage and slippage within the grips during testing (Figure 3b).

a) b

Figure 3. Test setup: a) universal testing machine; b) specimen gripping system

This device consists of two flat strips with rounded edges at each end of the specimen. Each end of the specimen is wrapped between the two flat strips, thereby reducing the risk of fracture at the grip edges (see Figure 3b).

For tensile loading, the upper crosshead of the tes–ting machine moved vertically upward. In accordance with laboratory procedures and industrial standard requirements, the specimens were preloaded with a force of 1□N, and the extension rate was set to 10□mm/ min. Each specimen was subjected to uniaxial tensile loading with a steadily increasing force until fracture occurred.

3. RESULTS AND DISCUSSION

3.1 Influence of the induced slit length

Figure 4 shows the force-displacement curve of the non-slit specimen. As can be observed, the uncracked speci–mens exhibited high fracture force (exceeding 2000□N) and a large displacement to failure of over 30□mm.

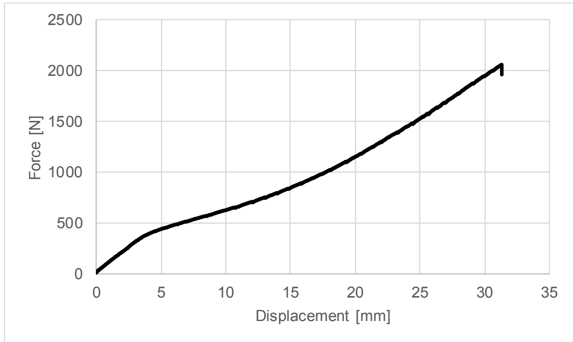

Figure 4. Force-displacement curve for the non-slit specimen

Figure 5 presents the force-displacement curves for different horizontal slit lengths across the specimen width, to illustrate the influence of these upon the uni–axial tensile strength.

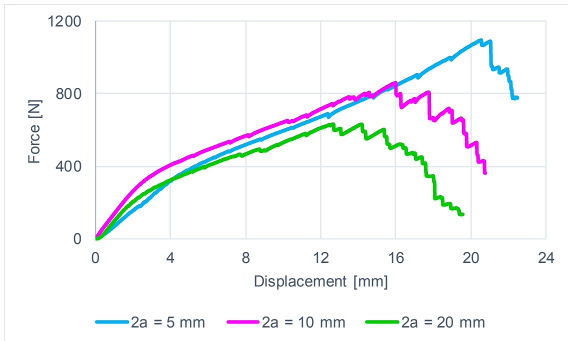

Figure 5. Force-displacement curves according to the horizontal slit lengths

The curves in Figure 5 exhibit the same shape up to the onset of crack propagation. Analysis of the tearing evolution shows that small „drops" (zig-zag patterns) appear in the ascending portion, which are attributed to the detachment and fracture of the filament bundles (see Figure 1d) within the coated fabric. Compared to the non-slit specimens, both the fracture forces and displacements are lower. This reduction is due to the decreased number of filaments that are going to break before complete specimen failure.

Figure 5 also demonstrates that the presence of a crack significantly affects the maximum load the coated textile material can withstand. Moreover, it is evident that the maximum tensile force decreases considerably with increasing initial crack length, and the slopes of the force-displacement curves diminish as the initial crack length increases.

Analysis of Figure 5 indicates that for small crack lengths (2a=5 mm), a very small plateau appears on the force–displacement diagram, suggesting an almost brittle fracture behavior, similar to that of the uncracked specimen. For larger initial crack lengths (2a=10 mm and 2a=20 mm), an extended plateau is observed in the force-displacement diagram, indicating a more ductile fracture behavior.

Thus, for slits longer than 10 mm (2a>10 mm), a more pronounced plastic deformation region emerges. The maximum forces obtained from testing specimens (Sp.1–Sp.5) with different initial horizontal crack lengths (2a=0, 5, 10, 20 mm) are presented in Table 2.

Table 2.Tearing forces obtained for non-slit (2a = 0) and slit induces specimens

Slit length [mm]	Maximum forces [N]						S.Dev [N]
	Sp. 1	Sp. 2	Sp. 3	Sp. 4	Sp. 5	Mean	
0	2050.6	1834.6	2002.1	2227.1	2060.8	2035.0	125.7
5	1076.0	1096.0	1033.3	1065.1	1060.5	1066.2	20.5
10	811.9	862.5	847.4	805.9	821.3	829.8	21.6
20	620.1	674.8	620.6	634.9	655.6	641.2	21.2

The differences between the recorded values (see Table 2) and the manufacturer's values (see Table 1) are below 20%, which considering the different testing and clamping conditions are comparable. Based on the standard deviation values, the results obtained for the maximum forces are acceptable. Similar standard devi–ation values are also observed for the cracked speci–mens. Figure 6 illustrates a nonlinear the tendency of the failure force when comparing the specimens altogether (non-slit and slit).

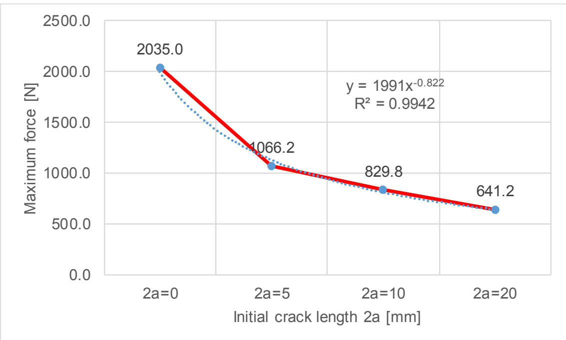

Figure 6. Maximum force vs. induced slit length

Figure 6 shows that increasing the crack length leads to a decrease in the maximum load the tarpaulin can withstand. An empirical correlation was fitted to the experimental data in order to quantify the observed reduction in maximum force with increasing slit length. Within the investigated range of slit lengths (2a = 5–20 mm), the relationship can be approximated by Equation (1), with a coefficient of determination of $R^2 = 0.9942$. It should be noted that this expression is purely empirical and is intended only to describe the experi–mental trend for the investigated material and testing conditions. Therefore, extrapolation beyond the tested slit lengths should be performed with caution.

$$F(2a) = 1991.0 \cdot (2a)^{-0.822} \tag{1}$$

Compared to the uncracked specimen, an initial crack length of 2a=5 mm reduces the maximum force by 47.6%, a crack length of 2a=10 mm reduces it by 59.2%, and a crack length of 2a=20 mm reduces it by 68.5%. The relation (1) is valid for crack lengths $2a \in [5,20]$ mm and for tarpaulin S8210 only.

Figure 7 illustrates the influence of induces slit len–gth on the fracture energy of the specimen.

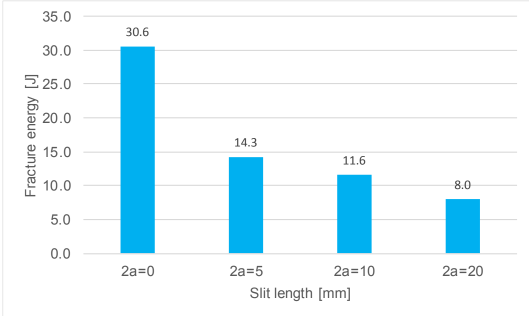

Figure 7. Effect of induces slit length on fracture energy

Increasing the initial crack length leads to a decrease in the fracture energy that the specimen can withstand. This is expected, as a longer crack reduces the specimen ligament, consuming less energy to break the remaining intact filaments.

Compared to the non-slit specimen, a crack length of 2a=5 mm reduces the fracture energy by 53.4%, 2a=10 mm reduces it by 62.0%, and 2a=20 mm reduces it by 73.8%. Thus, the larger the crack, the lower the fracture energy of the tarpaulin.

Figure 8 illustrates the influence of initial crack length on the energy corresponding to the maximum force. It is evident that, for the uncracked specimen, the energy corresponding to the maximum force is approximately equal to the total fracture energy of the specimen.

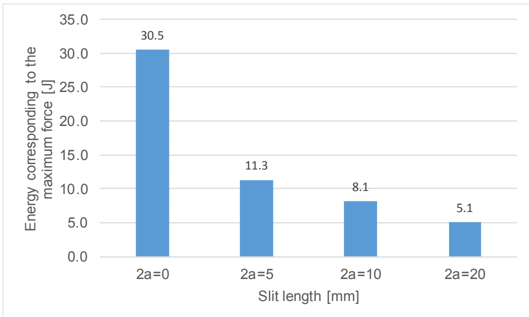

Figure 8. Effect of induced slit length on the energy corresponding to the maximum force

Figure 8 shows that increasing the initial crack len–gth leads to a decrease in the energy corresponding to the maximum force. It can be observed that, for the cracked specimens, the energy corresponding to the maximum force is lower than the total fracture energy of the specimen.

3.2 Failure mechanism of specimens with induces slit

To determine the fracture mechanism of specimens with different initial crack lengths, their failure behavior was monitored during the increase of the tensile load.

Figure 9 shows the crack propagation mode in spe–cimens containing an initial straight crack.

Analysis of the crack propagation shown in Figure 9 indicates that the evolution of the cracks occurs in three stages, namely:

➢ Crack opening stage – central crack specimen (Figure 9a): Under tensile loading, the initial crack develops into an elliptical shape, with its major axis perpendicular to the direction of the applied force (Figure 9b). In this stage, stress is concentrated at the crack tip, and the filament bundle near the crack tip begins to separate from the PVC coating layer.

➢Crack propagation stage: The load gradually increases and reaches the stress required to fracture the first filament at the crack tip, which breaks and transfers the load to the adjacent filaments (Figure 9c). The filaments behave as a nonlinear material, and a plastic zone gradually forms in the region adjacent to the crack. As the elliptical crack grows, the filament at the crack tip ruptures abruptly, and the adjacent filaments begin to slip alternately from the initial crack tip, with the first filament being pulled out (Figure 9d). During this stage, the filaments detach from the coating, generating friction between filaments and between the filaments and the coating, contributing to the reduction of the tarpaulin's tensile strength. If the applied load remains constant during this stage, the crack does not propagate further.

➢ Unstable crack propagation stage (specimen fracture): With increasing tensile load, the filaments near the crack tip break rapidly due to friction between the filaments and between the filaments and the coating. Consequently, the specimen can no longer carry any load, resulting in sudden fracture (Figure 9e).

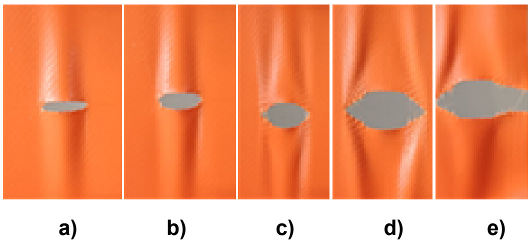

Figure 9. Crack propagation mechanism leading to final failure a) initial shape, b) elliptical shape, c) rupture of the first yarn, d) increase in the number of broken yarns, e) final rupture

All specimens with initial straight cracks underwent the three degradation stages described above, with the duration of the last two stages depending on the initial crack length, resulting in different fracture modes. For specimens with a larger initial crack ($2a \geq 10$ mm), the crack grows gradually, the propagation stage lasts longer, and the load decreases progressively until final fracture. In this case, the fracture is classified as progressive. For specimens with a smaller initial crack ($2a < 10$ mm), the propagation stage is very short, and the final fracture occurs abruptly, without noticeable crack growth; the degradation occurs mainly during the second crack propagation stage. In this case, the fracture is classified as brittle.

From a fracture-mechanics perspective, the decrease in maximum force and fracture energy with increasing slit length can be attributed to the reduction of the effective load-bearing ligament and the resulting increase in stress concentration at the crack tips. The fracture process is governed by several energy dissi–pation mechanisms, including filament rupture, pull-out of individual filaments from the PVC matrix, debonding between the yarns and the coating layer, and frictional sliding between adjacent filaments and yarns. The contribution of these mechanisms is evident from the progressive load drops observed in the force-displa–cement curves. As the initial slit length increases, a smaller number of intact yarns remain available to re–distribute the applied load, leading to earlier crack propagation and reduced fracture energy.

3.3 Influence of slit orientation on the failure force and energy

For the testing of specimens with inclined cracks, the specimens had an initial crack length of 2a=20 mm, and the cracks were oriented at θ =30°, 45°, and 60° relative to the horizontal direction (see Figure 2c). The force-displacement curves for individual specimens with cracks oriented at θ=30°, 45°, and 60° are presented in Figure 10.

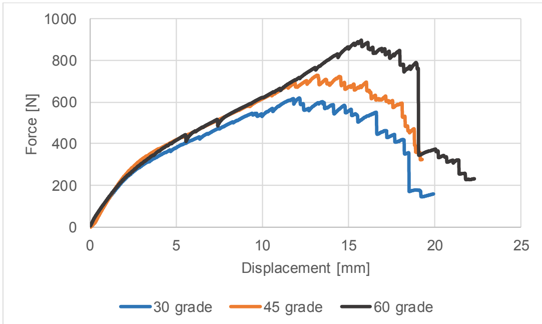

Figure 10. Force-displacement curves for crack orienta–tions at θ = 30°, 45°, and 60° (2a = 20 mm)

As with straight cracks, the curves also exhibit small „drops" (zig-zag patterns), caused by the detachment and fracture of the filament bundles forming the warp and weft.

Regardless of the crack orientation, the diagrams in Figure 10 show that both the force and displacement decrease as the crack angle decreases. The reduction in force at smaller angles can be explained by the fact that at a lower angle (30°) relative to the horizontal, a larger number of filaments are broken compared to a higher angle (60°). However, the influence of crack orientation cannot be attributed solely to the number of interrupted filaments. The tested tarpaulin possesses a strongly anisotropic architecture consisting of orthogonally woven warp and weft yarns embedded in a PVC coating. Consequently, the crack orientation affects not only the number of load-bearing yarns intersected by the slit but also the stress redistribution mechanisms within the woven structure. Different crack orientations modify the local load-transfer paths between adjacent yarns and alter the relative contributions of yarn stretching, yarn pull-out, yarn–coating debonding, and frictional sliding. As a result, specimens with identical crack lengths but different crack orientations exhibit different residual strengths and energy absorption capacities.

Based on the test results, the maximum force values for the tested specimens (Sp.1-Sp.5), with an initial crack length of 2a=20 mm and oriented at angles θ=30°, 45°, and 60° relative to the horizontal crack direction, are presented in Table 3.

Table 3. Maximum forces obtained for specimens with crack length 2a = 20 mm and different angles relative to the horizontal direction

Slit angle θ (°)	Fracture force (N)						S.Dev. (N)
	Sp. 1	Sp. 2	Sp. 3	Sp. 4	Sp. 5	Mean	
0	2050.6	1834.6	2002,1	2227.1	2060.8	2035.0	125.7
30	658.9	646.8	704.7	697.2	619.9	665.5	31.7
45	812.3	766.3	755.7	727.1	748.7	762.0	28.2
60	989.5	911.2	895.7	976.0	790.6	912.6	70.9

Based on the standard deviation values, the results obtained for the maximum forces are acceptable. Figure 11 illustrates the influence of crack angle on the fracture force for the same initial crack length (2a=20 mm).

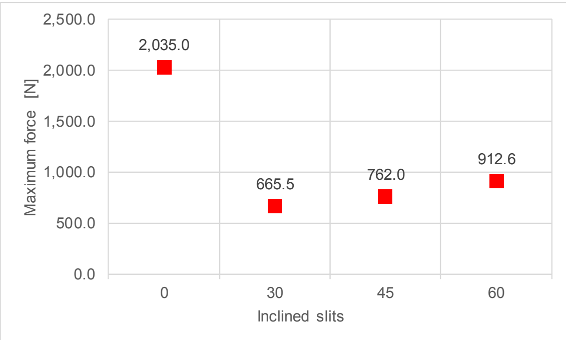

Figure 11. Effect of inclined slits on the maximum force

As shown in Figure 11, similar to horizontal cracks, the presence of an inclined crack reduces the maximum force that the tarpaulin can withstand. Compared to the uncracked specimen, a specimen with a crack inclined at **30°** reduces the maximum force by 67.3%, at **45°** by 62.6%, and at **60°** by 57.0%.

Figure 12 presents the variation of the maximum force as a function of crack inclination angle for specimens with a crack length of **2a=20 mm**, inclined at **θ =30°, 45°, and 60°.**

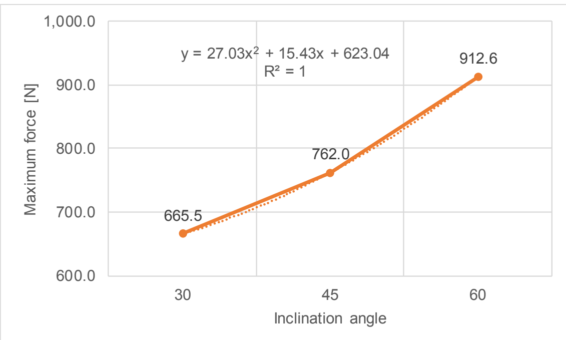

Figure 12. Variation of maximum force with crack inclination angle

Figure 12 shows that, for the same crack length (2a=20 mm) but different crack orientation angles, the force decreases as the inclination angle decreases. Using a polynomial function, the relationship between force and crack angle (θ) can be described by a polynomial function according to Equation (2), with a coefficient of determination of R^2=1. This relationship is valid for an initial crack length of 2a=20 mm and for cracks inclined relative to the specimen horizontal.

The polynomial relationship of Equation (2) should be interpreted as an empirical approximation of the measured data rather than a physically derived model. The equation is based on the tested crack orientations (30°, 45°, and 60°) and serves only to illustrate the inf–luence of crack inclination on the residual tensile stren–gth of the investigated material. Additional experi–mental data would be required to establish a generalized predictive model.

$$F(\theta) = 27.03\cdot(\theta)^2 + 15.453\cdot\theta + 623.04 \qquad (2)$$

Considering the 60° crack angle as a reference, for which the force reaches its maximum value (912.6 N), the maximum force of the specimen with a crack inc–lined at 45° is reduced by 16.5%, while for a crack inc–lined at 30° it decreases by 27.1%. This phenomenon can be explained by the number of intact filaments across the specimen width that carry the tensile load.

Figure 13 illustrates the influence of crack inclina–tion angle on the fracture energy of the specimen, with the crack having the same initial length (2a=20 mm).

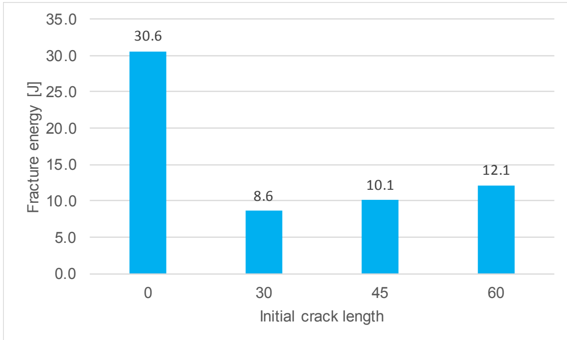

Figure 13. Effect of initial crack length on fracture energy

Figure 13 shows that, similar to straight cracks, an inclined crack reduces the fracture energy of the spe–cimen. For inclined cracks, the fracture energy decre–ases as the crack inclination angle decreases. This phe–nomenon occurs because, at higher inclination angles, the specimen ligament is reduced, requiring more energy to break the remaining intact filaments.

Compared to the uncracked specimen, a crack inclined at θ=30° reduces the fracture energy by 72.0%, θ=45° by 67.1%, and θ=60° by 60.4%.

Figure 14 illustrates the influence of crack inclination angle on the energy corresponding to the maximum force.

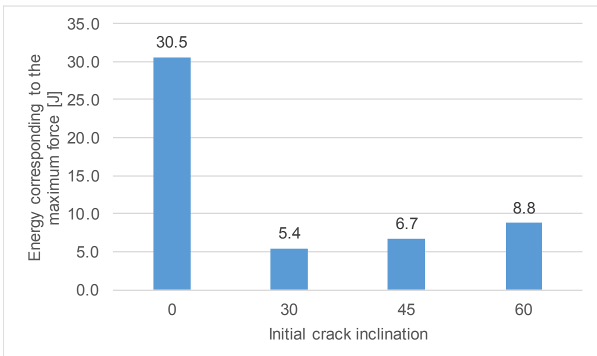

Figure 14. Effect of initial crack inclination angle on the energy corresponding to the maximum force.

Figure 14 shows that, for the same initial crack length (2a=20 mm) but different crack inclination angles relative to the horizontal, the energy correspon–ding to the maximum force decreases as the inclination angle decreases. In this case as well, the energy corresponding to the maximum force is lower than the total fracture energy of the specimen with the same initial crack length (2a=20 mm).

Considering 60° as the reference angle, for which the energy corresponding to the maximum force is highest (8.8 J), the energy at maximum force for a specimen with a crack inclined at 30° decreases by 38.1%, while for a crack inclined at 45° it decreases by 23.7%.

It is well known that individual filament failure promotes crack growth, so the number of filaments broken critically affects the tensile strength of the S8210 tarpaulin. Due to this, Bigaud et al. [10] proposed the concept of the equivalent initial crack length. By projecting the initial crack length (2a=20 mm) onto the axis perpendicular to the loading direction, the equivalent crack length is obtained (Figure 15), with the calculation relationship given as:

$$2a_{ech} = (2a)\cdot\cos\theta \qquad (3)$$

The equivalent crack lengths for cracks oriented at θ=30°, 45°, and 60° relative to the horizontal crack direction are presented in Table 4.

Table 4. Equivalent crack lengths at different angles relative to the horizontal

Initial crack length 2a [mm]	Equivalent crack length $2a_{ech}$[mm]		
	30^0	45^0	60^0
20	17.32	14.14	10.0

From the Tables 2 and 4, it can be observed that the specimen with a straight crack and an initial length of 2a=10 mm has an equivalent initial crack length of $2a_{ech}$=10 mm, identical to that of the specimen with a crack oriented at 60° and an initial crack length of 2a=20 mm.

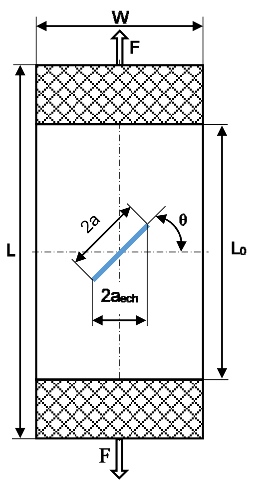

Figure 15. Definition of the equivalent crack length

Figure 16 presents the force–deformation curves for the two specimens (with horizontal and inclined cracks) having the same equivalent crack length (**$2a_{ech}$=10 mm**).

The similarity of the force-displacement responses shown in Figure 16 suggests that the equivalent crack length can successfully capture the combined influence of slit length and slit orientation on the tensile behavior of the investigated tarpaulin. Although the equivalent crack length concept has been previously proposed for textile-reinforced composites, the present results demonstrate its applicability to S8210 PVC-coated fabrics and indicate that it may be used as a practical parameter for estimating residual strength in damaged freight wagon tarpaulins. This observation is particularly relevant for maintenance practice, where defects of different orientations may be evaluated using a common damage descriptor. The differences between the two specimen forces-one with a straight crack (2a=10 mm) and the other with a crack inclined at 60° with a length of 2a=20 mm-are negligible, and up to a displacement of 15 mm, the two curves virtually overlap.

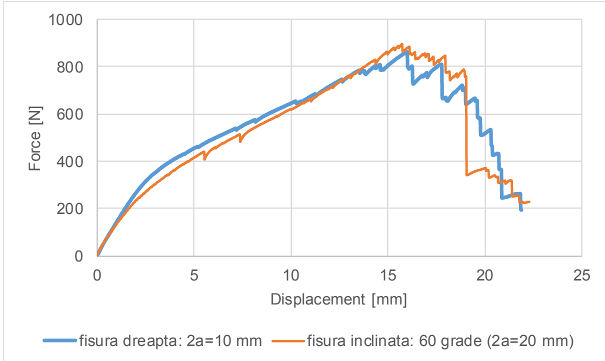

Figure 16. Fracture response at the same equivalent crack length

We also note that both shapes of the curves after the maximum force are following the same trend, the total displacement up to the specimen's ultimate failure being approximately the same.

From these data, it can be predicted that crack orientation and initial crack length can be combined into a single factor, called the equivalent initial crack length. Therefore, the equivalent crack length can represent the combined effect of both crack length and orientation relative to the applied force. Based on the conducted tests, the maximum forces were determined for the specimens with different initial crack lengths oriented horizontally, as well as for specimens with an initial crack length of 2a=20 mm and cracks oriented at θ=30°, 45°, and 60° relative to the horizontal crack direction.

These results of the maximum forces, are presented in Table 5.

Table 5. Maximum forces for specimens with different initial crack lengths and angles relative to the horizontal

Initial crack length (2a) [mm]	Crack angle (θ) [°]	Equivalent crack length ($2a_{ech}$) [mm]	Maximum force [N]
2a=5	θ=0°	$2a_{ech}$=5	1066.2
2a=10	θ=0°	$2a_{ech}$=10	829.8
2a=20	θ=0°	$2a_{ech}$=20	641.2
2a=20	θ=30°	$2a_{ech}$=17.32	665.5
2a=20	θ=45°	$2a_{ech}$=14.14	762.0
2a=20	θ=60°	$2a_{ech}$=10.00	912.6

Figure 17 illustrates the influence of the equivalent initial crack length on the maximum fracture force.

The relationship between the force (F) and the equivalent crack length (a_{ech}) can be described as a linear function according to Equation (4), with a coefficient of determination of R^2=0.9704.

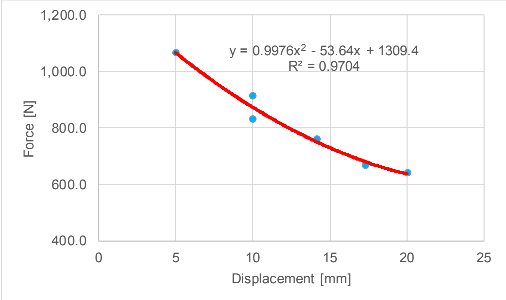

Figure 17. Force-equivalent crack length curve

It provides an empirical correlation between maxi–mum force and equivalent crack length for the tested S8210 tarpaulin specimens. Although the equivalent crack length has a physical interpretation as a measure of the effective reduction of the load-bearing ligament, the mathematical form of the fitted equation itself has no direct fracture-mechanics basis. Consequently, the relationship should be regarded as a material-specific engineering correlation valid only within the inves–tigated range of crack lengths and crack orientations.

$$F\left(a_{ech}\right) = 0.9976 \cdot a_{ech}^{2} - 53.64 \cdot a_{ech} + 1309.4 \quad (4)$$

The data from Table 5 and the trend of the curve shown in Figure 17 indicate that, in this case as well, the force decreases with increasing equivalent initial crack length. At the same time, the results show that cracks inclined relative to the tarpaulin's horizontal axis are less critical than straight cracks of the same length parallel to the horizontal axis. In practice, it is evident that cracks may occur in random orientations during service.

3.4 Fracture mechanism of specimens with inclined slits

To determine the fracture type of specimens with an initial crack length of 2a=20 mm and different crack orientations, their behavior was monitored during the increase of tensile load.

Figure 18 shows the crack propagation mode in specimens containing an initial inclined crack.

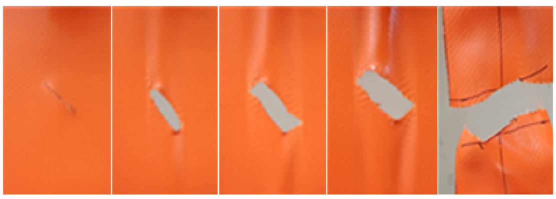

a) b) c) d) e)

Figure 18. Propagation mechanism of inclined cracks leading to final failure: (a) initial shape; (b) elliptical shape; (c) rupture of the first thread; (d) increase in the number of broken threads; (e) final rupture

The influence of crack orientation reflects the aniso–tropic nature of the woven tarpaulin architecture. Beca–use the load is transferred through orthogonal warp and weft yarns, inclined slits intersect different numbers of load-bearing yarns depending on their orientation. Con–sequently, the crack-tip stress field and the local load redistribution mechanisms differ from those observed for horizontal slits. The observed Z-shaped crack path indicates a mixed-mode fracture process involving both tensile opening and shear deformation. However, crack propagation ultimately tends to align perpendicular to the loading direction, following the preferential failure path imposed by the woven reinforcement structure. This behavior is consistent with the anisotropic fracture response reported for coated textile composites.

As with straight cracks, the propagation of inclined cracks can also be divided into three stages: the crack opening stage (Figures 18a and 18b), the crack propa–gation stage (Figures 18c and 18d), and the unstable crack propagation stage (specimen fracture) (Figure 18e). It is observed that, regardless of the inclination angle, the crack always propagates from the crack tip and develops perpendicular to the loading direction. This behavior is due to the orthogonal weaving pattern of the tarpaulin filaments.

The observed crack trajectories (figure 18) indicate that inclined slits are subjected to a mixed-mode loading condition involving both crack opening (Mode I) and in-plane shear (Mode II) [11]. In contrast to horizontal slits, where the fracture process is predominantly go–verned by tensile opening, inclined slits experience additional shear-induced deformation that promotes local yarn rotation, yarn sliding, and stress redistribution within the woven network. The interaction between opening and shear deformation contributes to the prog–ressive reorientation of the crack path toward a direction perpendicular to the applied load (Figures 9b and 18b). This behavior reflects the anisotropic nature of the woven reinforcement, which constrains crack growth along preferential paths defined by the warp and weft architecture. The resulting Z-shaped fracture pattern is therefore not only a geometric consequence of the initial slit orientation but also a manifestation of the coupled Mode I–Mode II fracture process and the anisotropic load-transfer mechanisms within the coated fabric.

3.5 Practical implications for repair assessment

Although EN 12641-1:2019 does not establish repair criteria for the tarpaulin membrane itself, it considers that load-bearing components associated with tarpaulin systems, such as ropes and webbings, may experience a reduction of approximately 20% in nominal strength during service due to wear and weathering. In the present study, this value was adopted as a conservative engineering reference for assessing the severity of slit-induced damage.The residual strength ratio was defined as:

$$R = \frac{F_{\max}}{F_0}$$

where Fmax is the maximum force of the damaged specimen and F0 is the average maximum force of the undamaged specimen. For the tested material, F0 = 2035 N, corresponding to a reference strength level of 1628 N for R = 0.8. Experimental results indicate that specimens containing a 5 mm slit exhibited an average maximum force of 1066 N, corresponding to a residual strength of only 52.4%.Therefore, all investigated slit configurations produced strength losses exceeding the 20% reference level.

These findings suggest that slit defects of approximately 5 mm and larger may significantly compromise the load-carrying capacity of the S8210 tarpaulin and should therefore be considered for inspection and repair. Nevertheless, this recommendation should be regarded as a material-specific engineering guideline rather than a universally applicable repair criterion, since service conditions, environmental degradation, safety factors, and loading history were not considered in the present study.

4. CONCLUSION

This study investigated the influence of slit length and orientation on the tensile fracture behavior of S8210 PVC-coated tarpaulin used for freight wagon coverings.

1. Both slit length and slit orientation significantly affect the residual tensile strength and fracture energy of the material. Increasing slit length and decreasing slit angle led to a reduction in load-carrying capacity and energy absorption.
2. The fracture process is governed by the anisotropic woven architecture of the tarpaulin and by micromechanical damage mechanisms, including yarn rupture, filament pull-out, yarn–coating debonding, and frictional sliding. Straight slits fail predominantly in Mode I, whereas inclined slits exhibit mixed-mode (Mode I/Mode II) crack propagation and a characteristic Z-shaped fracture path.
3. Two failure modes were identified for straight slits: abrupt fracture for short slits ($2a < 10$ mm) and progressive fracture for longer slits ($2a \geq 10$ mm), associated with different crack propagation behaviors.
4. The equivalent crack length concept successfully combines the effects of slit length and orientation and provides a practical parameter for estimating the residual strength of damaged S8210 tarpaulins.
5. Using the 20% strength reduction adopted in EN 12641-1:2019 for load-bearing tarpaulin-system components as an engineering reference level, all investigated slit configurations resulted in residual strengths below the corresponding 80% reference value. These results indicate that slit defects of approximately 5 mm and larger may significantly compromise the structural integrity of the investigated tarpaulin and should therefore be considered for inspection and repair.
6. The proposed force–slit relationships should be regarded as empirical engineering correlations valid for the investigated material and testing conditions. Their applicability outside the tested range of slit-lengths and orientations requires additional experimental validation.

ACKNOWLEDGMENT

This research received no external funding.

REFERENCES

[1] https://sioline.com/media/pages/db-databases/datasheets/d3f06be0ad-1733323707/s8210_en.pdf.

[2] Pirvulescu, L.D., Stoia, D.I., Marsavina, L., *Studies on Tensile and Tear Fracture of the S8210 tarpaulin*, JVE International, Vol. 46, 2022, 80-85.

[3] Bridgens, B.N., Gosling, P.D., *Direct stress-strain representation for coated woven fabrics*, Comput Struct 2004, 82, 1913–1927.

[4] Dinh, T.D., Rezaei, A., De Laet, L., Mollaert, M., Van Hemelrijck, D., Van Paepegem, W., *A new elasto-plastic material model for coated fabric*, Eng. Struct. 71 (2014), 222–233.

[5] Zhang, Y., Xu, J., Zhou, Y., Zhang, Q., Wu, F., *Central tearing behaviors of PVC coated fabrics with initial notch*, Composite Structures 208, Elsevier, 2019; 618-633.

[6] Sun, X., He, R., Wu, Y., Wang, T., *Uniaxial tearing properties and the tearing residual strength models of PTFE coated fabric*. Structures 33, Elsevier, 2021, 1354-1364.

[7] Wang, F., Chen, Y., Liu, G., Guo, Z., Fu, G., *Experimental investigation and theoretical analysis of tear propagation of GQ-6 airship envelope*, J Ind Text. 2018, 48(1), 304–21.

[8] Lanlan, Z., Yingying, Z., Wei, S., Junhao, X., Jigang, X., *A nonlinear damage constitutive model of PVC coated fabrics*, Structures 30, Elsevier, 2021, 368-377.

[9] Bao, H., Wu, M., Zhang, X., *Study on tearing tests and the determination of fracture toughness of PVC coated fabrics*, Jurnal of Industrial Textiles, Vol. 51(6), 2022, 977-1006.

[10] Bigaud, D., Szostkiewicz, C., Hamelin, P.,*Tearing analysis for textile reinforced soft composites under mono-axial and bi-axial tensile stresses*. Compos Struct. 2003;62 (2):129–37.

[11] Dumitru, I., Marsavina, L., *Introduction to fracture mechanics*, Publisher Mirton, Timisoara, 2001 (romana).

[12] Purnomo, Putu H. Setyarini, Agus D. Anggono, Fiber Orientation Effect on Fracture Toughness of Silk Fiber-Reinforced Zeolite/HDPE Composites, FME Transactions 49, pag. 128-134, 2021.

[13] Saboktakin A., Vu-Khanh T., Butun V., Pantyukhov P., Characteristics of Tufted Preforms Subjected to Different Mechanical Loading for Aerospace Applications, FME Transactions 46, Pag. 224-229, 2018

[14] Saghafi, H., Brugo, TM., Zucchelli, A., Fragassa, C., Minak G., *Comparison the effect of preload and curvature of composite laminate under impact loading*, FME Transactions, Vol. 44, No 4, pp. 353-357, 2016

[15] Dinulović, M., Rašuo, B., Krstić, B., Bojanić, A., *3D random fiber composites as a repair material for damaged honeycomb cores*, FME Transactions, Vol. 41 No 4, pp. 325-332, 2013.

[16] Funari, M. F., Spadea, S., Lonetti, P., Lourenço, P. B., *On the elastic and mixed-mode fracture properties of PVC foam*, Theoretical and Applied Fracture Mechanics 112 102924, 2021.

[17] Zhang, X., Zhou, Y., Wu, M., Li, Y., Bao, H., *Fracture toughness Gc of coated fabric with nonlinear tensile behaviors considered*, Construc–tion and Building Materials 415, 135007, 2024.

[18] Yu, Y, Cao, Z., Sun, Y., Mechanical properties of four types of PVC-coated woven fabrics at high-temperature and after exposure to high-temperature, Structures 33, Pag. 830–840, 2021.

[19] Guo, S., Wang, L., Shao, G., Shao, H., Jiang, J., Chen, N., Mechanical Behavior and Energy Dissipation of Woven and Warp-Knitted PVC Membrane Materials under Multistage Cyclic Loading, MDPI Polimers, 2022.

УТИЦАЈ ОРИЈЕНТАЦИЈЕ И ДУЖИНЕ ПРОРЕЗА НА ПОНАШАЊЕ КИДАЊА S8210 КОЈИ СЕ КОРИСТИ ЗА ЦЕРАДЕ ТЕРЕТНИХ ВАГОНА

Л. Д. Пирвулеску, Д. И. Стоиа, И. Бордеасу

Тканине обложене ПВЦ-ом се широко користе у церадама због своје издржљивости и флекси–билности. Ова студија истражује понашање кидања узорака тканине обложене ПВЦ-ом који садрже централне равне и косе прорезе, узорковане са церада типа S8210 које се користе у теретним ваго–нима. Једноосни тестови затезања су изведени и на нетакнутим и на прорезима. Анализирани су хори–зонтални прорези дужине 5, 10 и 20 мм, као и коси прорези од 20 мм под угловима од 30°, 45° и 60°. Резултати откривају два различита начина лома: прогресивни и нагли отказ. Коси прорези су пока–зали прогресиван образац ширења пукотине у об–лику слова Z, док хоризонтални прорези доводе до наглијег отказа. Одређени су кључни параметри лома, укључујући максималну силу лома, енергију лома и утицај геометрије прореза на чврстоћу лома. Такође је идентификована критична дужина отвора након које се препоручује поправка цераде. Рад преводи теоријске концепте енергије ломљења у директно мерљиви параметар (aech). Ово може дир–ектно испитати на лицу места особље за одржавање и на основу очитавања и предложених табела за овај материјал, може доносити безбедносне одлуке.